

Stability and Elastic, Electronic, and Thermodynamic Properties of $\text{Fe}_2\text{TiSi}_{1-x}\text{Sn}_x$ Compounds

JU-YONG JONG ^{1,2,4} JIHONG YAN,^{1,5} JINGCHUAN ZHU,³
and CHOL-JIN KIM^{2,3}

1.—School of Mechatronics Engineering, Harbin Institute of Technology, Harbin 150001, China. 2.—Department of Energy Science, Kim Il Sung University, Pyongyang, Democratic People's Republic of Korea. 3.—School of Materials Science and Engineering, Harbin Institute of Technology, Harbin 150001, China. 4.—e-mail: jjy429@163.com. 5.—e-mail: jyan@hit.edu.cn

We have systematically studied the structural, phase, and mechanical stability and elastic, electronic, and thermodynamic properties of $\text{Fe}_2\text{TiSi}_{1-x}\text{Sn}_x$ ($x = 0, 0.25, 0.5, 0.75, 1$) compounds using first-principles calculations. The structural and phase stability and elastic properties of $\text{Fe}_2\text{TiSi}_{1-x}\text{Sn}_x$ ($x = 0, 0.25, 0.5, 0.75, 1$) indicated that all of the compounds are thermodynamically and mechanically stable. The shear modulus, bulk modulus, Young's modulus, Poisson's ratio, electronic band structure, density of states, Debye temperature, and Grüneisen parameter of all the substituted compounds were studied. The results show that Sn substitution in Fe_2TiSi enhances its stability and mechanical and thermoelectric properties. The $\text{Fe}_2\text{TiSi}_{1-x}\text{Sn}_x$ compounds have narrow bandgap from 0.144 eV and 0.472 eV for Sn substitution from 0 to 1. The calculated band structure and density of states (DOS) of $\text{Fe}_2\text{TiSi}_{1-x}\text{Sn}_x$ show that the thermoelectric properties can be improved at substituent concentration x of 0.75. The lattice thermal conductivity was significantly decreased in the Sn-substituted compounds, and all the results indicate that $\text{Fe}_2\text{TiSi}_{0.25}\text{Sn}_{0.75}$ could be a new candidate high-performance thermoelectric material.

Key words: Full-Heusler, Fe_2TiSi , Fe_2TiSn , $\text{Fe}_2\text{TiSi}_{1-x}\text{Sn}_x$, thermoelectric, first principles

INTRODUCTION

Solid-state thermoelectric (TE) energy conversion is a promising and useful technology for both electric power generation from waste heat and cooling of various electronic devices, and this technology is expected to play a fundamental role in solving today's energy and environmental issues.¹ At present, one of the most well-known thermoelectric materials used in thermoelectric cooling devices is Bi_2Te_3 -based alloy, having maximum ZT of around 1.² Other materials with high ZT , such as $\text{In}_4\text{Se}_{3-\delta}$, filled skutterudite antimonides, $\text{AgPb}_m\text{Sb-Te}_{2+m}$, Tl-doped PbTe , and Ag_9TlTe_5 , have also been studied recently as next-generation advanced

thermoelectric materials.^{3–8} However, these compounds include toxic and scarce elements such as tellurium, antimony, and thallium, so it is important to develop new materials that consist of predominantly abundant and nontoxic elements and that can be obtained using relatively uncomplicated fabrication techniques. Fe_2XY Heusler compounds are good candidates for use in thermoelectric applications, and theoretical investigations have been carried out on Fe-based Heusler compounds using first-principle calculations, yielding power factors 4 to 5 times larger than those of classical thermoelectric materials at room temperature.⁹ Among these compounds, Fe_2VAl with Heusler-type structure is one of the most prominent examples because of its high thermoelectric power factor, and this material has been studied by many scientists.^{10–12} Fe_2TiSn and Fe_2TiSi compounds,

(Received February 28, 2017; accepted April 28, 2017; published online May 10, 2017)

which also belong to the group of Fe₂XY Heusler compounds, are promising candidate nontoxic and inexpensive thermoelectric materials, and previous theoretical investigations have shown that they possess high Seebeck coefficient from $-300 \mu\text{V K}^{-1}$ to $-160 \mu\text{V K}^{-1}$ around room temperature.¹³ The electronic structure and magnetic properties of Fe₂TiSn and Fe₂TiSi have been studied theoretically, and their physical and thermoelectric properties including elastic and electronic properties, electrical conductivity, Seebeck coefficient, as well as thermal conductivity studied.^{14–20} The Heusler compound Fe₂TiSi is confirmed experimentally to be a semiconductor with gap of 0.4 eV, having potential for use in thermoelectric applications.¹⁴ Lue et al. observed a Seebeck coefficient for Fe₂TiSn at around 340 K compatible with that of Fe₂VAI (at 300 K),¹⁵ and Shin et al. predicted that the temperature dependence of the thermoelectric properties can be tuned by substitution with Si. However, no reports are available on Fe₂TiSi_{1-x}Sn_x in literature, except for $x = 0$ and 1. To enhance the thermoelectric performance of Fe₂TiSi and Fe₂TiSn, we calculated and systematically studied the structural, phase, and mechanical stability as well as the elastic, electronic, and thermodynamic properties of Fe₂TiSi_{1-x}Sn_x ($x = 0, 0.25, 0.5, 0.75, 1$) compounds. The results indicate that Sn substitution at $x = 0.75$ in Fe₂TiSi improves the thermoelectric performance by adjusting the bandgap and significantly decreasing the lattice thermal conductivity. Our results are not only interesting from a fundamental point of view but could also be significant in the search for new candidate high-performance full-Heusler thermoelectric materials.

COMPUTATIONAL PROCEDURES

The crystal structure of Fe₂TiX (X = Si, Sn) is in space group *Fm-3m* (no. 225). There are 16 atoms in the unit cell of the Heusler compounds Fe₂TiX (X = Si, Sn). The Ti and Si atoms occupy two face-centered cubic (fcc) sublattices with origin at 4a (0, 0, 0) and 4b (1/2, 1/2, 1/2), respectively. The Fe atoms are located on 8c (1/4, 1/4, 1/4) sublattices, and each Fe atom has four Ti and four X atoms as nearest neighbors, while each Ti and X atom is surrounded by eight Fe atoms. For the nonstoichiometric compounds Fe₂TiSi_{1-x}Sn_x ($x = 0, 0.25, 0.5, 0.75, 1$), we used a conventional unit cell with 16 atoms (i.e., Fe₈Ti₄X₄), where alloying was performed by partial substitution of Si atom by Sn. This substitution was tested at four different sites of Si atom in the crystal by calculating the total energy for each case, but the difference was negligible and did not affect the results. The total energy, electronic structure, and elastic properties of the materials were studied using the Cambridge Serial Total Energy Package (CASTEP),²¹ based on density functional theory (DFT) in the generalized gradient approximation (GGA) with the Perdew–Burke–

Ernzerhof (PBE)²² exchange–correlation potential. All calculations were continued until the maximum force on atoms was below 0.01 eV/Å, the maximum displacement between cycles was below 5.0×10^{-4} Å, and the energy change was below 5.0×10^{-6} eV/atom. Periodic boundary conditions were applied, enabling expansion of the crystal wavefunction in terms of a plane-wave basis set. After a series of tests, the cutoff energy was set as 360 eV and the ultrasoft pseudopotential was chosen to describe the interaction of electrons between valence states and core states with the electron configurations for Fe, Ti, Si, and Sn atoms represented as $3d^6 4s^2$, $3s^2 3p^6 3d^2 4s^2$, $3s^2 3p^2$, and $5s^2 5p^2$, respectively. We used $8 \times 8 \times 8$ **k**-points according to the Monkhorst–Pack scheme²³ in the Brillouin zone for integrations, based on the Broyden–Fletcher–Goldfarb–Shanno (BFGS)²⁴ minimization technique. For a given atomic arrangement, the lattice parameters and atom positions were optimized to minimize the total energy, and the system was considered to have reached the ground state via self-consistent calculation when the total energy was stable within 5×10^{-7} eV/atom. We used a quasiharmonic Debye model to obtain the thermodynamic properties.

RESULTS AND DISCUSSION

Stability and Elastic Properties

We theoretically calculated the lattice constant of Fe₂TiSi_{1-x}Sn_x ($x = 0, 0.25, 0.5, 0.75, 1$) by minimizing the total energy using first-principle calculations; the optimized lattice constant for Fe₂TiSi and Fe₂TiSn is 5.658 Å and 6.032 Å, respectively (Table I). The differences from experimental results are smaller than 1%,^{14,25} indicating that the present calculations are highly reliable. If thermodynamic effects on the crystal structure are considered, our calculation results should be in good agreement with experimental results, and we can conclude that the computational parameters and conditions selected in this study are therefore suitable.

The enthalpy of formation, which determines the bulk stability of a compound, is defined as the difference between its total energy and the sum of the total energies of its constituents in their corresponding proportions. Generally, negative enthalpy of formation implies that the structure is thermodynamically stable, while a positive value means that the structure is unstable. To investigate the thermodynamic stability of Fe₂TiSi_{1-x}Sn_x ($x = 0, 0.25, 0.5, 0.75, 1$), the enthalpy of formation was calculated as

$$\Delta H_{\text{Fe}_8\text{Ti}_4\text{Si}_n\text{Sn}_{4-n}} = (E_{\text{Fe}_8\text{Ti}_4\text{Si}_n\text{Sn}_{4-n}}^{\text{tot}} - 8E_{\text{Fe}}^{\text{bulk}} - 4E_{\text{Ti}}^{\text{bulk}} - nE_{\text{Si}}^{\text{bulk}} - (4-n)E_{\text{Sn}}^{\text{bulk}}) / 16, \quad (1)$$

where $E_{\text{Fe}_8\text{Ti}_4\text{Si}_n\text{Sn}_{4-n}}^{\text{tot}}$ is the total energy of the compound Fe₈Ti₄Si_nSn_{4-n}, and $E_{\text{Fe}}^{\text{bulk}}$, $E_{\text{Ti}}^{\text{bulk}}$, $E_{\text{Si}}^{\text{bulk}}$,

Table I. Calculated lattice constant (a), substitution enthalpy of formation (ΔH), and density (d) of $\text{Fe}_2\text{TiSi}_{1-x}\text{Sn}_x$ ($x = 0, 0.25, 0.5, 0.75, 1$)

x	a (Å)			ΔH	d (g/cm ³)
	This work	Exp.	Ref.		
0	5.658	5.72 ¹⁴	5.685 ¹³	-0.64	6.878
0.25	5.758			-0.76	7.314
0.5	5.831			-0.87	7.713
0.75	5.939			-0.99	8.101
1	6.032	6.074 ²⁵	6.032 ¹³	-1.15	8.144

Table II. Elastic constants C_{11} , C_{12} , C_{13} , C_{33} , C_{44} , and C_{66} of $\text{Fe}_2\text{TiSi}_{1-x}\text{Sn}_x$ ($x = 0, 0.25, 0.5, 0.75, 1$)

x	C_{11}	C_{12}	C_{13}	C_{33}	C_{44}	C_{66}
0	462.4	124.5	124.5	462.4	152.0	152.0
0.25	423.7	125.1	125.1	423.7	145.8	145.8
0.5	388.6	113.0	121.8	392.0	141.3	139.1
0.75	367.1	120.2	120.2	367.0	132.2	132.2
1	345.1	119.4	119.4	345.0	118.1	118.1

and $E_{\text{Sn}}^{\text{bulk}}$ are the total energies of the pure elements in their bulk state; n is 4, 3, 2, 1, and 0 for $x = 0, 0.25, 0.5, 0.75,$ and 1, respectively. The enthalpy of formation for the $\text{Fe}_2\text{TiSi}_{1-x}\text{Sn}_x$ ($x = 0, 0.25, 0.5, 0.75, 1$) compounds is summarized together with their optimized ground-state lattice parameter and density in Table I.

It is clear that the enthalpy of all the $\text{Fe}_2\text{TiSi}_{1-x}\text{Sn}_x$ ($x = 0, 0.25, 0.5, 0.75, 1$) compounds was negative, confirming the thermodynamic stability of these structures. The lattice parameter and density increased with increasing x , indicating greater thermodynamic stability with increasing Sn substitution.

The elastic properties of a material are amongst the most important physical properties related to its structure and mechanical stability, in addition to some other fundamentally important properties. We therefore studied the elastic properties of the substituted compounds with different amounts of substitution of Si by Sn atoms. According to the unit cell of Fe_2TiSi , we chose substituent concentrations of $x = 0.25, 0.5,$ and 0.75 in $\text{Fe}_2\text{TiSi}_{1-x}\text{Sn}_x$, corresponding to one, two, or three Si atoms substituted by Sn atoms in the Fe_2TiSi unit cell. For $x = 0.5$, the primitive cell of $\text{Fe}_2\text{TiSi}_{0.5}\text{Sn}_{0.5}$ contains six atoms and has tetragonal structure in space group $P4/mmm$ (no. 123). The elastic constants C_{ij} for the $\text{Fe}_2\text{TiSi}_{1-x}\text{Sn}_x$ ($x = 0, 0.25, 0.5, 0.75, 1$) compounds as obtained from ground-state total energy calculations are presented in Table II.

There are five independent elastic constants at $x = 0.5$ due to the tetragonal symmetry, while the other compounds ($x = 0, 0.25, 0.75,$ and 1) have only three independent elastic constants. None of the C_{ij}

values are negative. The conditions for mechanical stability of cubic crystals at equilibrium are traditionally expressed in terms of the elastic constants as follows: $C_{11} > 0, C_{33} > 0, C_{44} > 0, C_{66} > 0, (C_{11} - C_{12}) > 0, (C_{11} + C_{33} - 2C_{13}) > 0, [2(C_{11} + C_{12}) + C_{33} + 4C_{33}] > 0$. The calculated elastic constants in Table III show that the $\text{Fe}_2\text{TiSi}_{1-x}\text{Sn}_x$ ($x = 0, 0.25, 0.5, 0.75, 1$) compounds are mechanically stable according to these stability criteria.

One can therefore calculate the other mechanical properties for these materials using the Voigt–Reuss–Hill (VRH) approximation. From the calculated elastic constants, the shear modulus G , bulk modulus B , and Young's modulus E can be estimated as follows: $B = (B_V + B_R)/2, G = (G_V + G_R)/2,$ and $E = 9BG/(3B + G)$, where $B_V, B_R, G_V,$ and G_R can be calculated as follows²⁶:

$$B_V = [2(C_{11} + C_{12}) + C_{33} + 4C_{13}]/9, \quad (2)$$

$$B_R = [(C_{11} + C_{12})C_{33} - 2C_{13}^2]/(C_{11} + C_{12} + 2C_{33} - 4C_{13}), \quad (3)$$

$$G_V = [M + 3C_{11} - 3C_{12} + 12C_{44} + 6C_{66}]/30, \quad (4)$$

$$G_R = 15/\{(18B_V/C^2) + [6/(C_{11} - C_{12})] + 6/C_{44} + 3/C_{66}\}, \quad (5)$$

$$M = C_{11} + C_{12} + 2C_{33} - 4C_{13}, \quad (6)$$

$$C^2 = (C_{11} + C_{12})C_{33} - 2C_{13}^2.$$

The calculated shear modulus G , bulk modulus B , and Young's modulus E are presented in Table III.

Table III. Bulk modulus B , shear modulus G , Young's modulus E , B/G , and Poisson's ratio of $\text{Fe}_2\text{TiSi}_{1-x}\text{Sn}_x$ ($x = 0, 0.25, 0.5, 0.75, 1$)

x	B	G	E	B/G	ν
0	237.1	158.6	389.0	1.496	0.221
0.25	224.6	147.2	362.5	1.526	0.231
0.5	209.2	138.5	340.3	1.511	0.229
0.75	202.5	128.6	318.4	1.574	0.238
1	194.6	116.0	290.2	1.679	0.251

The obtained values also obey the cubic stability condition: $C_{12} < B < C_{11}$, suggesting mechanical stability. Generally, the Young's modulus of a material is used to characterize its stiffness; materials with higher E are stiffer. Furthermore, the ratio of the bulk to shear modulus of crystalline phases can also predict their brittle or ductile behavior. Higher (lower) B/G ratio corresponds to ductile (brittle) behavior, the critical value which separates ductile from brittle materials being around 1.75. The values in Table III show that the $\text{Fe}_2\text{TiSi}_{1-x}\text{Sn}_x$ compounds become more ductile with increasing Sn substitution. We also calculated the Poisson ratio of the materials, as listed in Table III. This ratio can be used to quantify the stability of a crystal against shear, with most materials having values between 0.0 and 0.5. The Poisson ratio values of these materials reveal that the $\text{Fe}_2\text{TiSi}_{1-x}\text{Sn}_x$ compounds are mechanically stable and that their stability against shear is not weak. All these results confirm that Sn substitution is advantageous to enhance the stability and mechanical properties of these compounds.

Electronic Properties

The features of the band structure near the Fermi level determine the thermoelectric properties of a material, which are very useful to obtain reliable transport property values for thermoelectric materials. To theoretically investigate the electronic properties of the $\text{Fe}_2\text{TiSi}_{1-x}\text{Sn}_x$ ($x = 0, 0.25, 0.75, 1$) compounds, band-structure calculations were performed, as shown in Fig. 1.

As shown in Fig. 1, the electronic band structures of the $\text{Fe}_2\text{TiSi}_{1-x}\text{Sn}_x$ compounds show similar trends, but their conduction-band bottom shifted away from the Fermi level as the Sn content x was decreased. The $\text{Fe}_2\text{TiSi}_{1-x}\text{Sn}_x$ compounds are semiconductors with flat band at the bottom of the conduction band along G-X direction. The valence-band maximum and conduction-band minimum (at the G point) mainly consist of Fe 3d (t_{2g}) orbitals and Fe 3d (e_g) orbitals, respectively. The bandgaps in these band structures are well consistent with previous results of 0.144 eV for Fe_2TiSn and 0.472 eV for Fe_2TiSi .^{13,14} Figure 2 illustrates the change in the bandgap with the substituent concentration x .

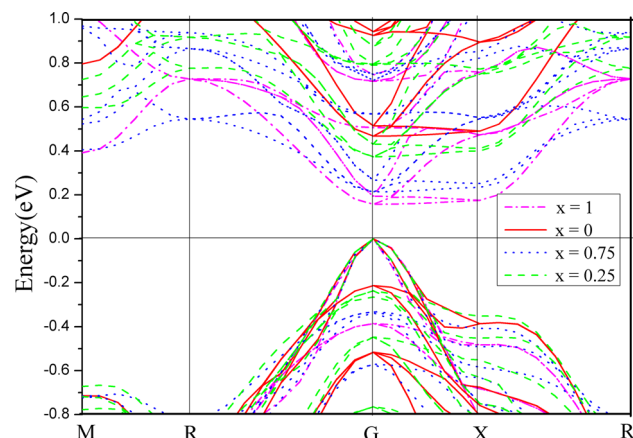
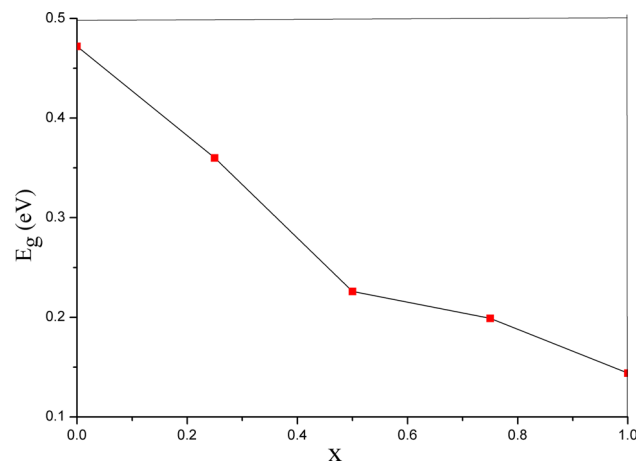
Fig. 1. Band structures of $\text{Fe}_2\text{TiSi}_{1-x}\text{Sn}_x$ ($x = 0, 0.25, 0.75, 1$).Fig. 2. Bandgap of $\text{Fe}_2\text{TiSi}_{1-x}\text{Sn}_x$ versus substituent concentration x .

Figure 2 shows that the $\text{Fe}_2\text{TiSi}_{1-x}\text{Sn}_x$ compounds have narrow bandgap values from 0.144 eV and 0.472 eV for Sn content ranging from 0 to 1. In previous research, the temperature dependence of the Seebeck coefficient S for different bandgaps was studied for Fe_2TiSi and Fe_2TiSn materials,¹³ indicating that the absolute S value at 300 K was stable and did not change when the bandgap was wider than 0.2 eV. As shown in Fig. 2, this condition is satisfied for substituent

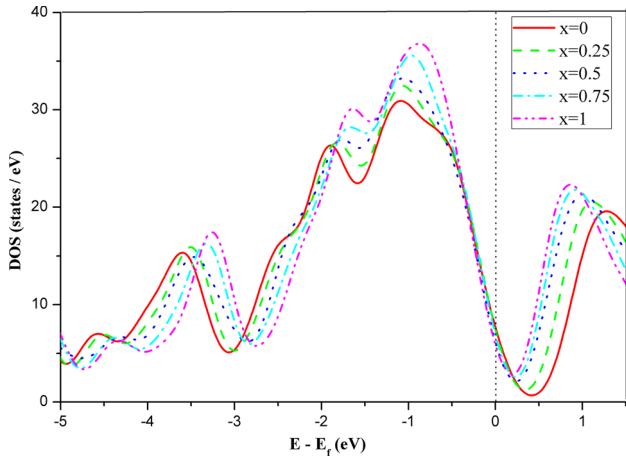


Fig. 3. Total density of states (TDOS) of $\text{Fe}_2\text{TiSi}_{1-x}\text{Sn}_x$ ($x = 0, 0.25, 0.5, 0.75, 1$).

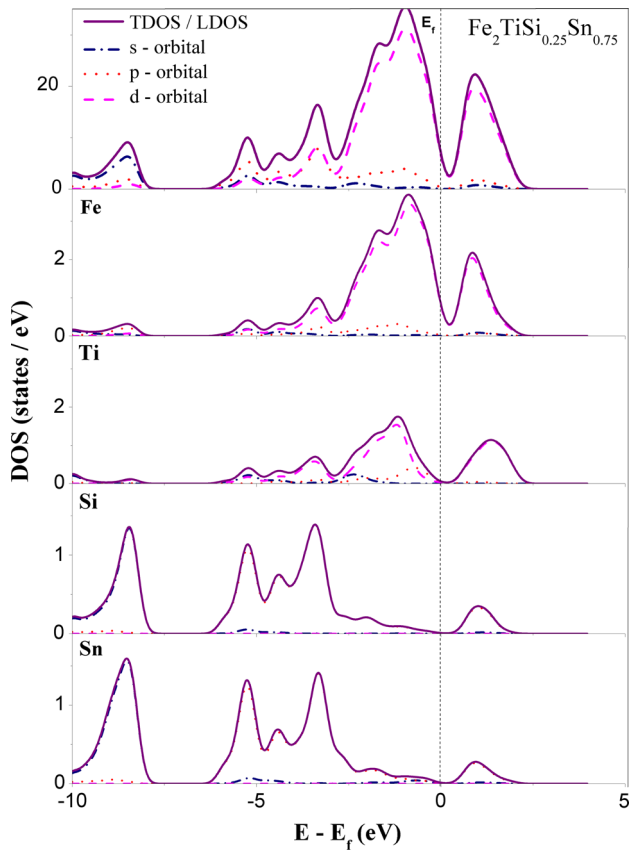


Fig. 4. DOS and PDOS of $\text{Fe}_2\text{TiSi}_{0.25}\text{Sn}_{0.75}$.

concentration of 0.75 or less. For deeper understanding of the electronic properties, the total and partial densities of states (TDOS and PDOS) were investigated. The total density of states (TDOS) near the Fermi level for the $\text{Fe}_2\text{TiSi}_{1-x}\text{Sn}_x$ compounds is shown in Fig. 3. Figure 4 presents the total DOS, local density of states (LDOS), and

partial densities of states (PDOS) of the $\text{Fe}_2\text{TiSi}_{0.25}\text{Sn}_{0.75}$ compound near the Fermi level.

The pattern of the DOS distribution of the $\text{Fe}_2\text{TiSi}_{1-x}\text{Sn}_x$ ($x = 0, 0.25, 0.5, 0.75, 1$) compounds is almost the same, but the detailed energy peak and band regions are not. The main contributions to the DOS near the Fermi level of these materials come from the d orbitals of Fe and Ti. The calculated band structure and DOS predict that these compounds have electronic structure with a narrow pseudogap at the Fermi energy. Lower DOS at the Fermi level and steeper DOS will lead to larger Seebeck coefficient according to the Mott approximation.²⁷ In $\text{Fe}_2\text{TiSi}_{1-x}\text{Sn}_x$ ($x = 0, 0.25, 0.5, 0.75, 1$) compounds, the slope of the DOS between the Fermi level and band top is slightly larger when x is bigger, and the DOS at the Fermi energy decreases slightly as the Sn substituent concentration x is increased. The calculated band structure and DOS of the $\text{Fe}_2\text{TiSi}_{1-x}\text{Sn}_x$ ($x = 0, 0.25, 0.5, 0.75, 1$) compounds show that the thermoelectric properties could be improved for substituent concentration x of 0.75.

Thermodynamic Properties

To improve the performance of thermoelectric materials, they should have large figure of merit $ZT = S^2T\sigma/\kappa$, where σ , S , T , and κ are the electrical conductivity, Seebeck coefficient, absolute temperature, and thermal conductivity, respectively.^{1,2} Therefore, to investigate whether a material could be a candidate for use in thermoelectric applications, one needs to investigate its thermal conductivity. The total thermal conductivity of a material includes both electronic thermal conductivity and lattice thermal conductivity. Previously reported experimental results show that the thermal conductivity of Fe_2TiSn mainly originates from the lattice component κ_l .¹⁵ Thus, a large reduction in κ_l is needed to enhance the thermoelectric performance. The lattice thermal conductivity can be obtained using the Debye temperature (Θ_D) and the Grüneisen parameter (γ) as²⁸⁻³³

$$\kappa_l(T) = \frac{0.617\theta_D^3 k_B^3 m V^{1/3}}{(1 - 0.514\gamma^{-1} + 0.228\gamma^{-2}) n h^3 \gamma^2 T}, \quad (7)$$

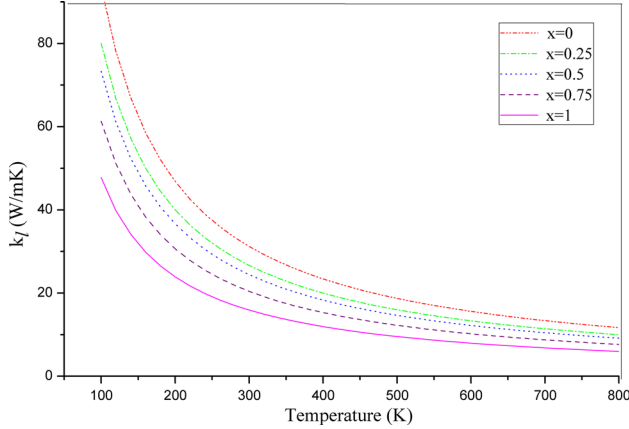
where n is the number of atoms in the unit cell, k_B is the Boltzmann constant, V is the volume of the unit cell, and m is the average atomic mass. If the elastic constants and electronic structures of the compound are known, one can estimate the Debye temperature and Grüneisen parameter from the average sound velocity using the following equations:

$$\theta_D = \frac{h v_m}{k_B} \left[\frac{3n}{4\pi} \left(\frac{\rho N_A}{M_m} \right) \right]^{\frac{1}{3}}, \quad (8)$$

$$\gamma = \frac{9}{2} \left(\frac{v_l^2 - 4v_t^2/3}{v_l^2 + 2v_t^2} \right), \quad (9)$$

Table IV. Calculated transverse (v_t), longitudinal (v_l), and mean sound speeds (v_m), Grüneisen parameter (γ), and Debye temperature (Θ_D) for Fe₂TiSi_{1-x}Sn_x ($x = 0, 0.25, 0.5, 0.75, 1$)

x	v_l (m/s)	v_t (m/s)	v_m (m/s)	γ	Θ_D (K)
0	8096.0	4813.4	5329.5	1.394	705.117
0.25	7586.5	4486.4	4970.0	1.413	647.181
0.5	7145.4	4237.0	4692.4	1.403	601.130
0.75	6794.6	3984.6	4417.5	1.444	557.703
1	6439.6	3710.4	4120.0	1.507	512.228

Fig. 5. Temperature-dependent lattice thermal conductivity of Fe₂TiSi_{1-x}Sn_x ($x = 0, 0.25, 0.5, 0.75, 1$).

where k_B is the Boltzmann constant, h is the Planck constant, ρ is the density of the material, N_A is Avogadro's number, and M_m is the molecular weight. v_m is the mean sound velocity, which can be calculated from v_l (longitudinal elastic wave velocity) and v_t (transverse elastic wave velocity), which are related to the bulk modulus and shear modulus by Navier's equation³⁴:

$$v_m = \left[\frac{1}{3} \left(\frac{2}{v_t^3} + \frac{1}{v_l^3} \right) \right]^{-\frac{1}{3}}, \quad v_l = \left(\frac{B + \frac{4G}{3}}{\rho} \right)^{\frac{1}{2}}, \text{ and} \\ v_t = \left(\frac{G}{\rho} \right)^{\frac{1}{2}}. \quad (10)$$

The calculated values of v_m , v_l , v_t , Θ_D , and γ for the Fe₂TiSi_{1-x}Sn_x ($x = 0, 0.25, 0.5, 0.75, 1$) compounds are presented in Table IV.

Based on the above formula, we calculated the lattice thermal conductivity of Fe₂TiSi_{1-x}Sn_x ($x = 0, 0.25, 0.5, 0.75, 1$) and show the results in Fig. 5.

The lattice thermal conductivity of Fe₂TiSi_{1-x}Sn_x ($x = 0, 0.25, 0.5, 0.75, 1$) decreases with increasing temperature. Fe₂TiSi has higher lattice thermal conductivity than Fe₂TiSn, due to the heavier Sn atoms. The κ_l values of the substituted compounds are lower than that of the pure compound, because

Sn substitution increases the phonon scattering centers. Our calculations are, of course, approximate and somewhat simplistic to clarify the precise thermodynamic properties of Fe₂TiSi_{1-x}Sn_x, but the tendencies can be considered to be reliable and supported with sufficient evidence.

CONCLUSIONS

We systematically studied the structural, phase, and mechanical stability as well as the elastic, electronic, and thermodynamic properties of Fe₂TiSi_{1-x}Sn_x ($x = 0, 0.25, 0.5, 0.75, 1$) compounds using first-principles calculations. The following conclusions can be drawn:

1. The structural and phase stability, and elastic properties (shear modulus, bulk modulus, Young's modulus, and Poisson's ratio) of the Fe₂TiSi_{1-x}Sn_x ($x = 0, 0.25, 0.5, 0.75, 1$) compounds were studied; the results indicate that all of the compounds are thermodynamically and mechanically stable, and Sn substitution in Fe₂TiSi enhances its stability and mechanical properties.
2. The electronic band structure, DOS, and charge density distribution were researched, indicating that the Fe₂TiSi_{1-x}Sn_x compounds have narrow bandgaps from 0.144 eV to 0.472 eV for Sn substitution ranging from 0 to 1. The calculated band structure and DOS of Fe₂TiSi_{1-x}Sn_x show that the thermoelectric properties could be improved at substituent concentration x of 0.75.
3. The thermodynamic properties of the Fe₂TiSi_{1-x}Sn_x compounds were studied, revealing that the lattice thermal conductivity was significantly decreased in the Sn-substituted compounds. All the results indicate that Fe₂TiSi_{0.25}Sn_{0.75} could be a new candidate high-performance thermoelectric material.

ACKNOWLEDGEMENTS

This work was supported by the National Natural Science Foundation of China (Grant No. 5141101303).

REFERENCES

1. T.M. Tritt, *Annu. Rev. Mater. Res.* 41, 433 (2011).

2. D.L. Zhao and G. Tan, *Appl. Therm. Eng.* 66, 15 (2014).
3. Y.B. Losovyj, L. Makinistian, E.A. Albanesi, A.G. Petukhov, J. Liu, P. Galij, O.R. Dveriy, and P.A. Dowben, *J. Appl. Phys.* 104, 083713 (2008).
4. H. Li, X. Tang, Q. Zhang, and C. Uher, *Appl. Phys. Lett.* 94, 102114 (2009).
5. K.F. Hsu, S. Loo, F. Guo, W. Chen, J.S. Dyck, C. Uher, T. Hogan, E.K. Polychroniadis, and M.G. Kanatzidis, *Science* 303, 818 (2004).
6. J.P. Heremans, V. Jovovic, E.S. Toberer, A. Saramat, K. Kurosaki, A. Charoenphakdee, S. Yamanaka, and G.J. Snyder, *Science* 321, 554 (2008).
7. K. Kurosaki, A. Kosuga, H. Muta, M. Uno, and S. Yamanaka, *Appl. Phys. Lett.* 87, 061919 (2005).
8. L.E. Bell, *Science* 321, 1457 (2008).
9. D.I. Bilc, H. Geoffroy, W. David, G.M. Rignanese, and P. Ghosez, *Phys. Rev. Lett.* 114, 136601 (2015).
10. Y. Nishino, S. Deguchi, and U. Mizutani, *Phys. Rev. B* 74, 115115 (2006).
11. M. Mikami, K. Kobayashi, T. Kawada, K. Kubo, and N. Uchiyama, *Jpn. J. Appl. Phys.* 47, 1512 (2008).
12. M. Mikami and M. Mizoshiri, *J. Electron. Mater.* 43, 1922 (2014).
13. Y. Shin, O. Masakuni, N. Akinori, Y. Kurosaki, and J. Hayakawa, *Appl. Phys. Expr.* 6, 025504 (2013).
14. M. Meinert, M.P. Geisler, J. Schmalhorst, U. Heinzmann, E. Arenholz, W. Hetaba, M. Stöger-Pollach, A. Hütten, and G. Reiss, *Phys. Rev. B* 90, 085127 (2014).
15. C.S. Lue and Y.K. Kuo, *J. Appl. Phys.* 96, 2681 (2004).
16. A. Jezierski and A. Słebarski, *J. Magn. Magn. Mater.* 223, 33 (2001).
17. S.V. Dordevic and D.N. Basov, *Phys. Rev. B* 66, 075122 (2002).
18. B. Xu and L. Yi, *J. Phys. D Appl. Phys.* 41, 095404 (2008).
19. J.Y. Jong, J. Zhu, S.I. Pak, and G.H. Sim, *J. Electron. Mater.* 45, 5104 (2016).
20. J.Y. Jong, J. Zhu, M.G. Jon, Y. Zhou, J. Kim, and J. Yan, *J. Alloys Compd.* 693, 462–467 (2017).
21. M.D. Segall, M.D. Segall, P.J.D. Lindan, M.J. Probert, C.J. Pickard, P.J. Hasnip, S.J. Clark, and M.C.J. Payne, *J. Phys. Condens. Matter* 14, 2717 (2002).
22. J.P. Perdew, K. Burke, and M. Ernzerhof, *Phys. Rev. Lett.* 77, 3865 (1996).
23. H.J. Monkhorst and J.D. Pack, *Phys. Rev. B* 13, 5188 (1976).
24. H. Fischer and J. Almlöf, *J. Phys. Chem.* 96, 9768 (1992).
25. A. Słebarski, *J. Phys. D Appl. Phys.* 39, 856 (2006).
26. R. Hill, *Proc. Phys. Soc.* 65, 349 (1952).
27. J.M. Buhmann and M. Sigrist, *Phys. Rev. B* 88, 115128 (2013).
28. G.A. Slack, *Solid State Phys.* 34, 1 (1979).
29. D. Wee, B. Kozinsky, B. Pavan, and M. Fornari, *J. Electron. Mater.* 41, 977 (2012).
30. L. Bjerg, B.B. Iversen, and G.K.H. Madsen, *Phys. Rev. B* 89, 024304 (2014).
31. C. Toher, J.J. Plata, O. Levy, M. de Jong, M. Asta, M.B. Nardelli, and S. Curtarolo, *Phys. Rev. B* 90, 174107 (2014).
32. G.A. Slack, *J. Phys. Chem. Solids* 34, 321 (1973).
33. B. Mayera, H. Antona, E. Botta, M. Methfesselb, J. Stichta, J. Harrisc, and P.C. Schmidta, *Intermetallics* 11, 23 (2003).
34. O.L. Anderson, *J. Phys. Chem. Solids* 24, 909 (1963).